Paper 131

©Civil-Comp Press, 2012
Proceedings of the Eleventh International Conference
on Computational Structures Technology,
B.H.V. Topping, (Editor),
Civil-Comp Press, Stirlingshire, Scotland

Experimental Analysis of the Dynamic Behaviour of Railway Turnouts

V.L. Markine[1] and I. Shevtsov[2]
[1]Faculty of Civil Engineering
Delft University of Technology, the Netherlands
[2]ProRail, Utrecht, the Netherlands

Abstract

The dynamic behaviour of turnouts is analysed using filed measurements from instrumented turnout crossings. The dynamic responses of each turnout arising from passing trains are measured using a mobile device. The main elements of the device are the three-dimensional acceleration sensor (to be installed at the crossing nose), the velocity sensor and the sleeper displacement sensor. The measured dynamic response of the turnout primarily comprise the accelerations of the crossing nose and the displacements of a sleeper recorded for the three dimensions.

Based on velocity of the passing trains (which is measured as well) the locations of the maximum accelerations of the crossing nose arising from each wheel are derived.

These locations indicate the most probable area for initiation of the fatigue defects on the crossing nose [5]. Moreover, depending on the direction and the magnitude of these accelerations regular and irregular wheel-rail contact in the turnout crossing can be detected. In [6] such data from an instrumented turnout have been used for validation of the numerical model.

Using the above-mentioned device a number of turnouts were measured. The dynamic responses were collected and analysed. Based on this analysis some conclusions about the effects of:

- the type and velocity of the passing trains;
- the type of turnout (e.g. crossing angle, sleeper material); and
- the vertical rail geometry (crossing nose)

on the performance of the turnout crossing (assessed by the magnitude and location of the wheel contact forces) are drawn. The results are presented and discussed.

Keywords: instrumented turnout, wheel/rail contact, crossing nose damage.

1 Introduction

Railway turnouts are important elements of the railway infrastructure, which enables trains to be guided from one track to another at a railway junction as shown in Figure 1.

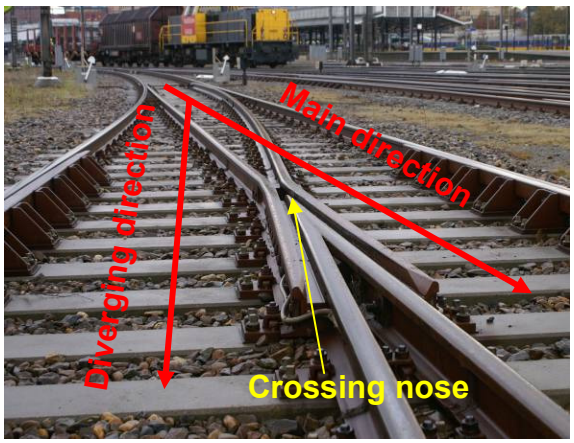

Figure 1 Railway turnout and crossing nose

In this figure it can clearly be seen that at the location of the crossing nose the rail geometry (the inner rail) is discontinuous. Due to such a discontinuity the crossing nose experiences high impact loads from the wheels of passing trains. These forces initiate various types of damage to the crossing nose of the railway turnout (Figure 2). Statistical evidence shows that failures in turnouts cause major operational disturbances in a railway network.

The train and turnout interaction has been analysed both numerically and experimentally in a number of research papers being published recently. Various numerical models for analysis of the dynamic behaviour of turnout can be found in [1]-[6]. Experimental analysis of the turnout behaviour is important as well. It was investigated in a number of papers usually for the purpose of numerical model validation [6]-[8].

Figure 2 RCF damage of crossing nose

In this paper the results of the measurements in the common crossing of turnouts are presented. The measurements were performed within the framework of the project investigating the effects of the vertical elasticity of turnout performance commissioned by ProRail (rail infrastructure provider in the Netherlands) [5]. In the first phase of this project the effects of the elastic elements (such as rail pads, under sleeper pads and ballast mats), vertical rail geometry and sleepers on the dynamic forces in the crossing nose were numerically investigated. The next step in this project was to verify the numerical findings using field measurement.

During the field tests the accelerations of the crossing nose and sleepers due to passing trains on different types of turnouts were measured. Other responses (e.g. fatigue areas on the crossing nose) were derived from the measured acceleration signals. Using the measurements some relationships between the types of the train, train velocities, crossing condition and type of sleepers on one hand and the forces in the crossing nose on the other were established.

The measurement device, the measured and derived data are described in Section 2. The results of the performed field tests are presented and discussed in Section 4. Conclusions are given in Section 5.

2 Instrumented crossing

The measurement device used here is designed for analysis of the wheel-rail contact in the crossing area. The device consists of

- The 3D acceleration sensor on a magnet which has to be placed at the side of the crossing nose (Figure 3)
- Two inductive sensors to be installed on the rail on before the crossing nose. Using the distance between the sensors the train velocity can be determined.
- The sleeper displacement sensor (optional) to be place on one of sleepers near the crossing nose
- The main unit, wherein all the signals are received and synchronised.

Figure 3 Acceleration sensor mounted on crossing nose

An example of the raw data i.e. the rail accelerations due to moving train is shown in Figure 4.

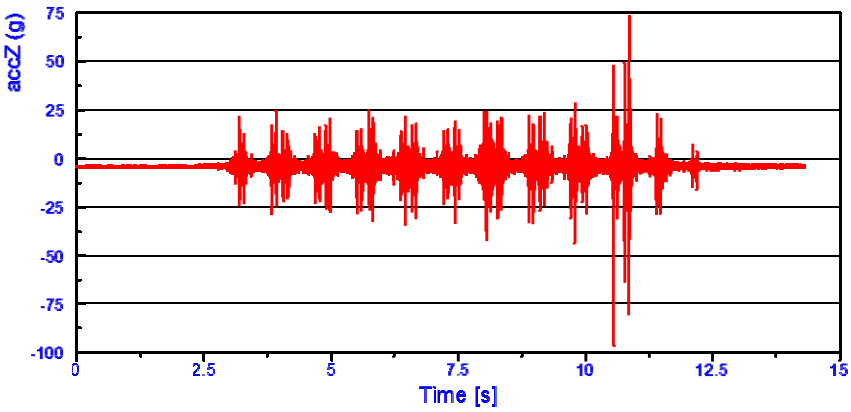

Figure 4 Rail accelerations (crossing nose)

Since the velocity of the passing train and the distance from the velocity sensor to the beginning of the crossing nose are known, it is possible to determine the magnitude and location of the maximum wheel force acting on the crossing nose. The locations of the maximum vertical accelerations of the crossing caused by each wheel, which presumably correspond to the locations of the first impact of the wheel, are presented as the wheel contact distribution histogram (Figure 5). The maximum accelerations are sought within 1m from the beginning of the crossing (point N) based on the wheels velocity and the distance between the velocity sensors and the point N as shown in Figure 5. Based on such a histogram the most probable area for fatigue damage (fatigue area) on the surface of the crossing nose can be determined.

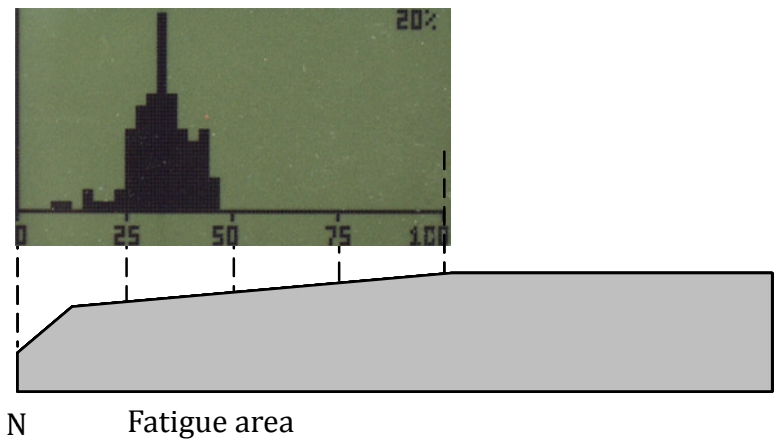

Figure 5 Wheel contact distribution in crossing nose

Other data used here, which is derived from the measured accelerations, is the maximum acceleration of the crossing nose caused by each wheel of the passing train. An example of such a plot is shown in Figure 6. In this figure the maximum vertical, lateral and total accelerations of the rail per wheel are shown. Based on this data the wheel forces can be estimated and the quality of each wheel can be assessed.

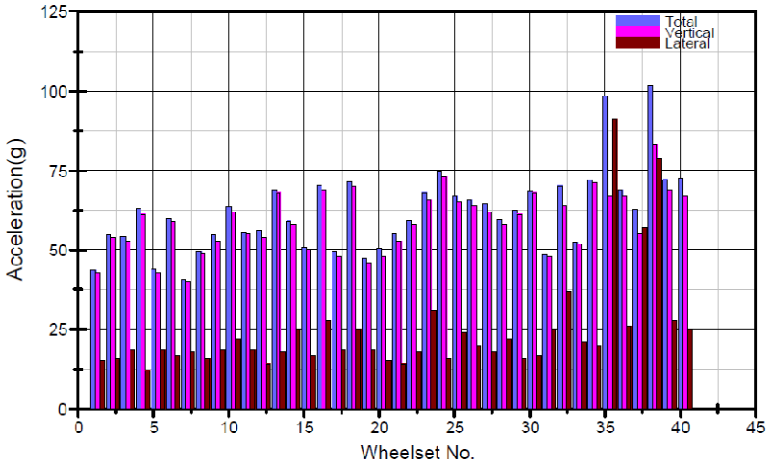

Figure 6 Maximum rail (crossing nose) accelerations due to wheels of passing train

3 Measurements

The measurements presented here were performed in three different locations in the Netherlands. The measured turnouts were with the angle 1:12 and 1:15 on concrete and wooden sleepers. The trains were passing these turnouts with the operational speed. An overview of the measured turnouts and the passed trains is given in Table 1.

Turnout	**Angle**	**Sleepers**	**Trains**	**Velocities [km/h]**
W1	1:15	Concrete	DDAR	39
			VIRM	39, 120, 130
W2	1:15	Wooden	DDAR	35
W3	1:12	Concrete	DDAR	90
			VIRM	80
W4	1:12	Concrete	DDAR	80
			VIRM	70
W5	1:15	Concrete	VIRM	120, 130, 135
			ICE	130

Table 1 Overview of measurement locations

To assess the performance of the measured turnouts (and the wheel quality of the passing trains) the following responses were obtained:

- Maximum vertical and lateral accelerations of the crossing due to passing wheels (contact forces)
- Wheel contact distribution (fatigue area) along the crossing nose
- Assessment of the wheel contact (regular or irregular and mark)
- Displacements of the sleeper.

Apart from the measured data from the instrumented turnouts the pictures of the rail surfaces were taken as well. The vertical geometry in the crossing nose obtained as well by manually measuring the distance from the top of the through rail to the crossing nose. The wear of the wing rail is taken into account as well. The measurement results are presented and discussed below.

4 Results and discussion

The measured results were collected and analysed. The complete overview of the measurements, conclusions and recommendations is presented in [8]. The main results and conclusions drawn from the measurements are presented below.

4.1 Effect of the vertical rail geometry

The measurement results have shown that the vertical geometry of the crossing nose has strong influence on the impact point distribution, i.e. the location and number of the fatigue areas (Figure 5) on the crossing nose. Usually, a new turnout with the theoretical geometry of the crossing nose has one area where most of the impact contacts are located (assuming that the wheels are of good quality). So that one of the measured turnouts W5 (1:15, Table 1), which was relatively new and the crossing nose vertical geometry was close to the theoretical one (Figure 7a) had the fatigue area on the distance 0.40m - 0.50m from the beginning of the crossing nose (Figure 7b), when the trains were passing with the speed of 130 km/h.

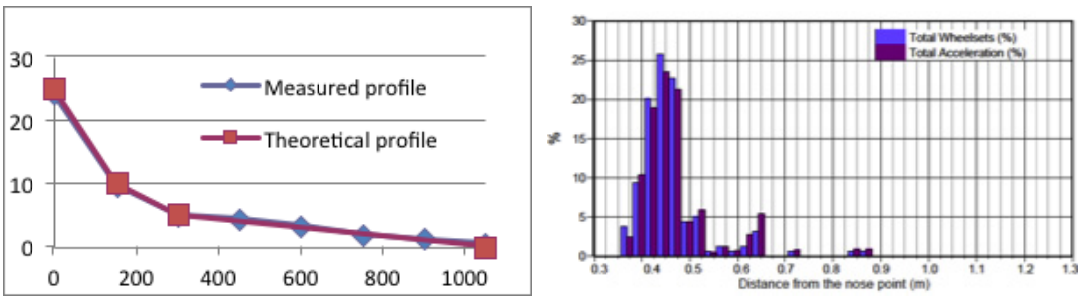

a. b.

Figure 7 Turnout W5 (Table 1) 1:15, relatively new, Vtrains= 130 km/h:
a. vertical geometry, b. wheel impact distribution

On the other hand, the turnout W1 (Table 1) with the same angle 1:15 and for the trains passing with the approximately same velocity (120-138 km/h) had two (instead of one) fatigue areas on the crossing nose, namely around 0.6m-0.7m and 0.9m-1.0m as shown in Figure 8b. The difference in the impact zones in the crossing nose of these two turnouts can be explained by the fact that the W1 turnout was recently repaired (welded) and the original (theoretical) geometry had not been restored, which can be seen from Figure 8a. This deviation in the rail geometry has resulted in that the impacts on the crossing nose occur later and in two different locations (Figure 8b). These results have shown that maintaining the crossing nose geometry is important for controlling the wheel-rail contact forces in turnout. Also these results have confirmed the numerical results obtained earlier in this project [10].

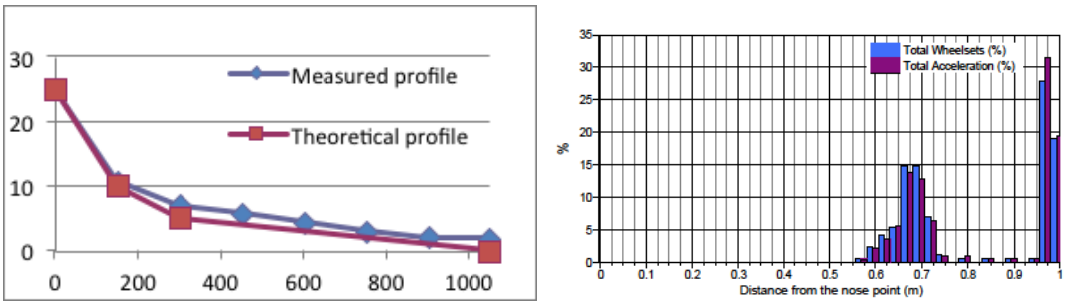

Figure 8 Turnout W1 (Table 1) 1:15, repaired, Vtrains= 120-138 km/h:
a. vertical geometry, b. wheel impact distribution

4.2 Effect of wooden sleepers

One of the measured turnouts W2 (Table 1) had wooden sleepers so that it was possible to compare its dynamic responses with the similar turnout on the concrete sleepers and to investigate the effect of the turnout vertical elasticity on the dynamic responses of the crossings. Since the turnout W2 was located close to the station the velocities of the passing trains were relatively low (35 km/h).

The comparison of the accelerations of the turnouts on the wooden and concrete sleepers is given in Table 2, from which it can be observed that the average accelerations of the turnout with concrete sleepers (W1) are the factor **3** higher than the accelerations for the turnout with wooden sleepers (W2). This means that increased elasticity of the crossing and low-weight sleepers reduce the contact forces in the crossing nose. This confirms the results of the numerical modelling from the previous step of this project presented in [5], [10].

4.3 Effect of vehicle and wheel condition

Using the measurements it was possible to analyse the effect of the different type of trains and the wheel quality on the dynamic responses (accelerations) of the crossing nose. Two types of the vehicle were compared, namely the VIRM and DDAR trains used by the Dutch Railways.

Turnouts	
W1, 1:15, **concrete** sleepers Vtrain = 37.9 km/h	W2, 1:15, **wooden** sleepers, Vtrain = 39.0 km/h
Vertical accelerations (average)	
Locomotive: 20.75 g Wagons: 21.85 g	Locomotive: 7.5 g Wagons: 8.5 g
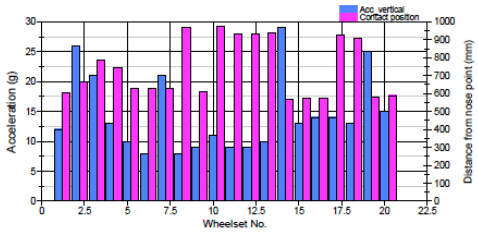	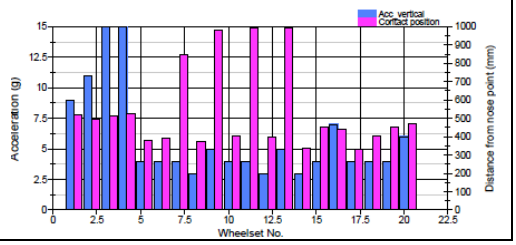

Table 2 Comparison of crossing nose accelerations for turnouts with wooden and concrete sleepers

Based on the measured accelerations it can be concluded that on the turnouts with the same angle and of the same condition the VIRM trains had a bit better defined fatigue area (the wheel contact distribution was narrower) than the DDAR trains as it is shown in Figure 9. Also the wheel-rail contact forces of the locomotives (the DDAR trains) were much higher (up to factor 3) than the forces of the wagons as it is Figure 10.

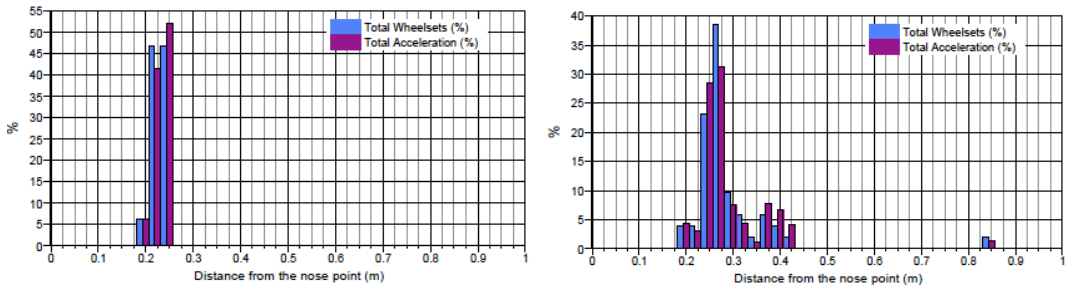

a. b.

Figure 9 Wheel impact contact distribution of crossing nose, turnouts W3/W4 (Table 1) due to: a. VIRM (35-80 km/h); b. DDAR (80-90km/h)

The high incidental impact accelerations observed in the measurement results were mostly due to bad wheels (valid for both the DDAR and VIRM trains) as it is shown in Figure 11. From the measurement results it was also observed that the vertical accelerations were usually much higher than the lateral ones, which means that the vertical forces are mostly responsible for damage to the common crossings.

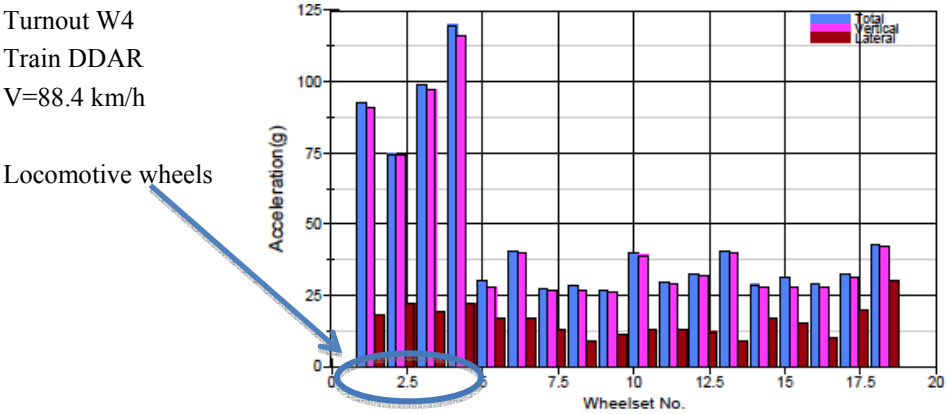

Figure 10 Impact forces due to locomotive and wagon wheels

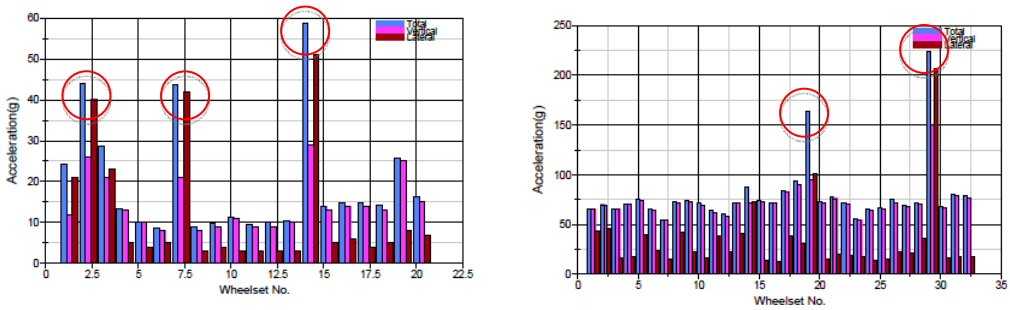

Figure 11 Incidental high impact forces due to bad wheels, turnout W1:
a. DDAR train (39 km/h), b. VIRM train (129 km/h)

5 Conclusions

The accelerations of the crossing nose of turnouts with the angle of 1:12 and 1:15 due to passing trains were measured (the VIRM, DDAR en ICE types). The vertical geometry in the crossing nose was obtained as well by manually measuring the distance from the wing rail to the crossing nose. Based on these measurements the impact distribution plots indicating the fatigue areas in the crossing nose for each passing wheel were obtained.

Based on the measured results it was concluded that the geometry of the crossing nose has strong influence on the location of the impact contact on the crossing nose and finally on its damage.

Also it could be seen that increasing vertical elasticity (by using the wooden sleepers) and reducing the sleeper weigh of the turnouts reduces the impact forces on

the crossing nose. Also the type of the passing trains, the axle load and the condition of the wheel strongly affect the dynamic forces on the crossing nose.

References

[1] Kassa, E., Andersson, C. and Nielsen, J.C.O. (2006) Simulation of dynamic interaction between train and railway turnout, Vehicle System Dynamics, March 2006, Vol. 44, No.3, pp. 247-258.

[2] Wiest, M., Daves, W., Fischer, F.D. and Ossberger, H. (2008) Deformation and damage of a crossing nose due to wheels passages. Wear, Vol. 265, pp. 1431-1438.

[3] Andersson, C. and Dahlberg, T. (2000) Load impacts at railway turnout crossing, Vehicle System Dynamics, 2000, vol. 33, SUPPL, pp. 131 – 142.

[4] Alfi, S. and Bruni, S. (2009) Mathematical modelling of train-turnout interaction, Vehicle System Dynamics, 47:5, 551- 574.

[5] Markine, V.L., Steenbergen, M.J.M.M. and Shevtsov, I.Y. (2011) Combatting RCF on switch points by tuning elastic track properties, *Wear* 271 (2011), pp. 158-167. doi:10.1016/j.wear.2010.10.031

[6] Wan, C., Markine, V.L. and Shevtsov, I.Y. (2012) Simulation of Train-Turnout Interaction and Validation using Field Measurements. In *Proceedings of the First International Conference on Railway Technology: Research, Development and Maintenance*, J. Pombo, (Editor), Civil-Comp Press, Stirlingshire, United Kingdom, paper 136, 2012. doi:10.4203/ccp.98.136

[7] Kassa, Elias and Nielsen, Jens C. O.(2008) 'Dynamic interaction between train and railway turnout: full-scale field test and validation of simulation models', Vehicle System Dynamics, 46: 1, 521 — 534. DOI: 10.1080/00423110801993144

[8] Cornish, A., Kassa, E. and R. Smith, R. (2012) Field Experimental Studies of Railway Switches and Crossings. In *Proceedings of the First International Conference on Railway Technology: Research, Development and Maintenance*, J. Pombo, (Editor), Civil-Comp Press, Stirlingshire, United Kingdom, paper 137, 2012. doi:10.4203/ccp.98.137

[9] Markine, V.L. (2012) Dynamic Response Measurements of Common Crossings. Research commissioned by ProRail. TU Delft report 7-12-234-03. ISSN 0169-9288

[10] Markine, V.L. and Steenbergen, M.J.M.M. (2009) Elasticiteit Wissels Op Betonnen Dwarsliggers. Rapportage fase 02, 04 van het onderzoek in opdracht ARCADIS/ProRail. TU Delft report 7-09-234-01. ISSN 0169-9288 (In Dutch)